

ORIGINAL ARTICLE

Plasmin cleavage of β 2-glycoprotein I alters its structure and ability to bind to pathogenic antibodies

Hannah F. Bradford¹  | Christophe J. Lalaurie²  | Jayesh Gor³ | Xin Gao³  |
 Charis Pericleous⁴  | Stephen J. Perkins³  | Hannah Britt³ |
 Konstantinos Thalassinos^{3,5}  | Ian Giles⁶  | Anisur Rahman⁶  |
 Mihaela Delcea⁷  | Paul A. Dalby²  | Thomas C. R. McDonnell²  

¹Division of Infection and Immunity, Institute of Immunity and Transplantation, Royal Free Hospital, University College London, London, United Kingdom

²Department of Biochemical Engineering, University College London, London, United Kingdom

³Division of Biosciences, Institute of Structural and Molecular Biology, University College London, London, United Kingdom

⁴Faculty of Medicine, National Heart and Lung Institute, Imperial College London, London, United Kingdom

⁵Institute of Structural and Molecular Biology, Birkbeck College, University of London, London, United Kingdom

⁶Division of Medicine, Centre for Rheumatology, University College London, London, United Kingdom

⁷Department of Biophysical Chemistry, Institute of Biochemistry, University of Greifswald, Greifswald, Germany

Correspondence

Thomas C. R. McDonnell, Department of Biochemical Engineering, University College London, 4th Floor Rayne Institute, 5 University Street, UCL, London WC1E 6JF, UK.
 Email: thomas.mcdonnell.11@ucl.ac.uk

Funding information

We thank the Medical Research Foundation for a fellowship to T.C.R.M. (MRF-057-0004-RG-MCDO-C0800) and a Versus

Abstract

Background: β 2-Glycoprotein I (β 2GPI) is the main autoantigenic target of antiphospholipid syndrome, with antibodies leading to clinical manifestations. There are 2 known structural isomers of β 2GPI: a J shape and a circular shape. The transition between these structures is incompletely understood, with the functional implications unknown. β 2GPI is a substrate of the protease plasmin, which cleaves within the fifth domain of β 2GPI, leading to altered cellular binding. Very little is currently known regarding the structure and function of this protein variant. We present the first comprehensive structural characterization of plasmin-clipped β 2GPI and the associated implications for pathogenic antibody binding to this protein.

Aim: To determine if cleavage of β 2GPI by plasmin triggers structural change, and what this change may mean for antibody reactivity.

Methods: β 2GPI was purified using an adapted acid-free process from healthy control plasma and cleaved with plasmin. Cleavage was confirmed by sodium dodecyl sulfate-polyacrylamide gel electrophoresis. Structural characterization was undertaken using dynamic light scattering, small-angle X-ray scattering, ion mobility mass spectrometry, and molecular dynamics simulation. Activity was tested using inhibition of β 2GPI enzyme-linked immunosorbent assays with patient samples and cleaved β 2GPI in the fluid phase and cellular binding by flow cytometry using human umbilical vein endothelial cells.

Results: Dynamic light scattering revealed a significantly smaller hydrodynamic radius for plasmin-clipped β 2GPI ($P = .0043$). Small-angle X-ray scattering and molecular dynamics analysis indicated a novel S-like structure of β 2GPI only present in the plasmin-clipped sample, while ion mobility mass spectrometry showed different structure distributions in plasmin-clipped compared with nonclipped β 2GPI. The

Manuscript handled by: Keith Neeves

Final decision: Keith Neeves, 11 February 2025

Hannah F. Bradford and Christophe J. Lalaurie share first authorship.

© 2025 The Author(s). Published by Elsevier Inc. on behalf of International Society on Thrombosis and Haemostasis. This is an open access article under the CC BY license (<http://creativecommons.org/licenses/by/4.0/>).

Arthritis Senior Fellowship (ShS/SRF/22977). H.F.B. was supported by a UCB BIOPHARMA SPRL/BBSRC PhD Studentship (BB/P504725/1). C.J.L. was supported by the Engineering and Physical Research Council (EPSRC) Centre for Doctoral Training in Emergent Macromolecular Therapies (000033549) and IPSEN Bioinnovation (EP/L015218/1). S.J.P. was supported by the CCP-SAS project, a joint EPSRC (EP/K039121/1), and National Science Foundation (CHE-1265821) grant. P.A.D. is supported by an EPSRC Grant (EP/P006485/1). Wellcome Collaborative Award in Science (209250/Z/17/Z) to K.T.

increased binding of autoantibodies was shown for plasmin-clipped β 2GPI ($P = .056$), implying a greater exposure of pathogenic epitopes following cleavage.

Conclusion: Cleavage of β 2GPI by plasmin results in the production of a unique S-shaped structural conformation and higher patient antibody binding. This novel structure may increase the production of antibodies and explain the loss of binding to phospholipids described previously for plasmin-clipped β 2GPI.

KEYWORDS

autoantigens, β 2-glycoprotein I, cleavage, plasmin, structural change

1 | INTRODUCTION

β 2-Glycoprotein I (β 2GPI) is a serum glycoprotein of approximately 50 kDa, comprised of 4 structurally similar domains (DI-DIV) and a structurally distinct fifth domain (DV), arranged in single chain-like beads on a string. β 2GPI circulates at a concentration of 200 μ g/mL and has been proposed to exist in 2 possible structures: an “open” J-shaped and a “circular” O-shaped structure [1]. The first 4 domains are members of the short complement regulator superfamily, termed DI to DIV, while the C terminal domain (DV) contains lysine-rich regions on the surface, responsible for cellular binding. The activities of β 2GPI widely vary from angiogenesis to complement activation, while the structure of β 2GPI is hypothesized to have significant implications for the activity of the molecule based on the assumption that, in the circular form, various motifs are hidden from solvent, thus preventing interactions with expected binding partners [1].

In circulation, β 2GPI has a number of contrasting functions and is almost unique [2] in being capable of both up- and downregulation of the complement and coagulation cascades. It is incompletely understood how these opposing functions are balanced; however, it has been hypothesized that regulation between these opposing functions is through structural restriction. Therefore, the structure of β 2GPI and the factors that modify it are crucial to fully understand its activity and function.

The structure of β 2GPI is complex, and as previously mentioned, it can form a linear (J-shaped; PDB ID: 1C1Z) or a circular (O-shaped) structure. However, it has been suggested that β 2GPI can also form an intermediate or alternative structure that is S-shaped, as first shown by Hammel et al. [3] using small-angle X-ray scattering (SAXS) [1,3–6]. The regulation of its structure is incompletely understood; however, several factors have been shown *in vitro* to trigger structural change, including changes in pH, salt concentration [1], disulfide reduction [7], and lysine acetylation [8]. Genetic manipulations to delete a disulfide to mimic the impact of reduction [9], although less clinically relevant, have also been shown by SAXS to associate with a linear structure. Most recently, Kumar et al. [10] studied the potential for a shift in serum concentration to purely linear β 2GPI, highlighting the potential for this equilibrium to be shifted and altering the exposure of protein motifs.

The role of β 2GPI in complement and coagulation is further complicated by the fact that it is a substrate for plasmin. β 2GPI plays a role in the conversion of plasminogen to plasmin, facilitating this through the binding of DV to plasminogen [11]. Plasmin is then capable of cleaving β 2GPI between the eighth and ninth amino acids from the C-terminus, yielding a peptide byproduct of 8 amino acids and a shortened DV. This modification of β 2GPI prevents its binding to plasminogen and thus slows the conversion of plasminogen to plasmin in the absence of other cofactors for plasminogen cleavage [12]. A change in activity post cleavage has also been shown in a number of other studies [13–15].

A complication in the study of plasmin-clipped β 2GPI is the nomenclature and various ways the protein is studied, with only a few studies confirming clipping by N-terminal sequencing [16]; in contrast, the majority of papers rely on functional testing to confirm modification [13,17]. Plasmin-clipped β 2GPI can act as an inhibitor of angiogenesis [13], a function much less prominent in the noncleaved form. Interestingly, angiogenesis is linked to both thrombosis and fibrinolysis in a wide range of settings where thrombin in a fibrin clot confers angiogenic properties to endothelial cells [18], while defective angiogenesis can delay thrombus resolution [19]. Therefore, an alteration in the angiogenic potential of β 2GPI may be through altering its activity in either thrombosis or fibrinolysis. Furthermore, the cleavage of β 2GPI leads to increased cardiac manifestations in neonatal lupus *in vivo* [14] due to the loss of the binding site for Ro60, an autoantigen linked to other autoimmune disorders that functions as an RNA scavenger. β 2GPI binds in the central pore of Ro60, blocking complexing with anti-Ro60 autoantibodies. This complex induces fetal heart block; therefore, β 2GPI binding is protective. Plasmin cleavage disrupts the DV of β 2GPI and thus prevents binding to Ro60. Plasmin-clipped β 2GPI has also been linked to cerebral infarction in antiphospholipid syndrome (APS) patients [15], while uncleaved β 2GPI has not been shown to have these same effects. Notably, Itoh et al. [20] showed increased levels of plasmin-clipped β 2GPI in leukemia patients, specifically associated with increased thrombosis, while Kim et al. [21] have shown structurally specific epitopes driving thrombosis that are yet to be evaluated in plasmin-clipped proteins. Despite this physiological role, the structures adopted by plasmin-clipped β 2GPI are yet to be elucidated.

β 2GPI is also the main autoantigenic target of APS. APS is an autoimmune clotting disorder that is the leading cause of strokes under 50 years old and recurrent miscarriage. Patients routinely develop autoantibodies to cardiolipin and β 2GPI, both of which feature in diagnostic clinical criteria; however, a number of noncriteria antibodies also exist. Several studies have placed significant importance on anti- β 2GPI autoantibodies, both diagnostically and mechanistically, as these antibodies are pathogenic in a range of mouse models [22,23]. Domain I (DI) contains a cryptic neo-epitope that has been defined (R39-G43) to which the most pathogenic anti- β 2GPI antibodies are formed, which have been shown to be thrombotic both *in vitro* and *in vivo*. Reversal agents that specifically target DI [24,25] have reduced clotting in *in vitro* functional assays and in both acute and chronic APS mouse models [26–28]. The formation of the anti- β 2GPI/ β 2GPI complex can trigger thrombosis in several ways, including through complement dysregulation [29]. The influence of the β 2GPI structure in APS is less well known, with few structural methods applied to β 2GPI from patient serum. The circular form of β 2GPI, traditionally hypothesized to be dominant in serum, theoretically hides both the DI and DV epitopes as well as the theoretical immunoglobulin (Ig) A epitopes visible in the linear forms [30], implying the requirement of an open β 2GPI form for antibody complex formation and thus disease progression [31]. That said, DV antibodies have recently been suggested not to be pathogenic [32], and the theory of requiring structural change for binding has been refuted by recent research [10]. The role of plasmin cleavage in APS is even less well studied, and given the role of β 2GPI in regulating both complement and coagulation and the role of these cascades in APS, a naturally occurring cleavage by these cascades on a regulator is interesting. For example, during thrombosis, β 2GPI may act as a cofactor, increasing this process and, in doing so, also, by proxy, activating complement and cleaving β 2GPI, which then loses the ability to regulate other functions. As such, it is vital to understand the structures formed by β 2GPI post plasmin cleavage to study the effect of plasmin-clipped β 2GPI in APS.

Here, we use a combination of biophysical and *in silico* techniques to characterize the structures of β 2GPI generated by plasmin cleavage and gain a better understanding of how the structures are formed and stabilized in solution (Supplementary Figure S1). The identification of novel structures may lead to an increased understanding of autoantibody generation, thrombosis formation, and how the structure of β 2GPI affects its role in various bodily systems.

2 | METHODS

2.1 | Purification of β 2GPI

Research samples were collected by written informed consent (National Research Ethics Committee- London Hampstead, reference number 12/LO/0373). A total of 50 mL of plasma was separated by SepMate as per manufacturer instructions (StemCell Technologies). β 2GPI was precipitated from plasma using a polyethylene glycol (PEG) precipitation method as previously described [33]. Briefly, plasma was diluted 1:4 with 10 mM sodium phosphate (pH 6.8), and 40% PEG 4000

(VWR) in 10 mM sodium phosphate (pH 6.8) was cooled on ice. The 40% PEG 4000 solution was then added dropwise to the diluted plasma while mixing on a magnetic plate. For 35 mL of plasma, 12.5 mL of 10 mM sodium phosphate was added, and a further 75 mL of PEG 4000 to a final concentration of PEG 4000 of 25% and incubated (4 °C for 30 minutes). Precipitate was collected in 50 mL Falcon tubes by centrifugation (3000 \times g for 30 minutes). The supernatant was discarded, and the precipitate was resolubilized in 20 mM Tris pH 8.0 at an appropriate volume. This was centrifuged (30 minutes, 3000 \times g) to remove insoluble matter, and the supernatant was taken forward to purification. Purification was initially across 3 \times 1 mL Heparin FF columns (Cytiva) at a flow rate of 1 mL/min. Samples were pump-loaded, and the pressure was kept below 0.3 mPa. Once loaded, the column was washed with 30 mL of 20 mM Tris pH 8.0. A gradient was used to purify β 2GPI between 30 mM NaCl and 350 mM NaCl, starting at 0% and finishing at 100% over 1 hour; 5 mL fractions were collected and checked for β 2GPI by sodium dodecyl sulfate-polyacrylamide gel electrophoresis (SDS-PAGE). Samples were then dialyzed (centrifugal concentration) or spiked into 50 mM sodium acetate, 50 mM NaCl, pH 4.5 (buffer A), and loaded on a 5 mL SP HP column (Cytiva). Samples were eluted across a gradient of 40% to 60% buffer B (50 mM sodium acetate, 650 mM NaCl, pH 5.3) over 1 hour, and peaks were checked for β 2GPI by SDS-PAGE. Peaks containing β 2GPI were pooled and purified by size exclusion chromatography (16/600, Superdex 200) in phosphate saline buffer (PBS) using a single isocratic wash. Samples were quantified by a bicinchoninic acid assay using a bovine serum albumin (BSA) standard curve. Curves from IEX pre and post cleavage are available in Supplementary Figure S5, comparative analysis of purified vs commercial protein is also available in Supplementary Figure S3.

2.2 | Proteomics

A portion of the β 2GPI stock solution (10 μ g) was lyophilized and resuspended in 50 mM ammonium bicarbonate (10 μ L). Samples were treated with 45 mM dithiothreitol (5 μ L) at 56 °C for 15 minutes, followed by alkylation with 10 mM iodoacetamide (5 μ L) at room temperature for 20 minutes in the dark. Sequencing grade trypsin was added to a 1:50 enzyme:protein ratio, and the sample was made up to 100 μ L with 50 mM ammonium bicarbonate and incubated overnight at 37 °C. The resulting peptides were enriched with C18 stage tips prepared in-house and eluted with 80% acetonitrile containing 0.5% acetic acid. The samples were dried down by SpeedVac (Thermo) and resuspended in 97% H₂O, 3% acetonitrile with 0.1% formic acid, and 10 fmol/ μ L Hi [4] *Escherichia coli* digest (Waters Corporation) for analysis by liquid chromatography mass spectrometry/mass spectrometry (MS).

Peptides resulting from trypsinization were analyzed in triplicate on a Synapt G2-Si QToF mass spectrometer connected to a NanoAcquity Ultra Performance UPLC system (both Waters Corp). The data acquisition mode used was mobility-enhanced MS^E over *mass over charge* ranging from 50 to 2000 with high energy collisional voltage in the transfer region ramped from 25 to 55 V. Mobile phases used for chromatographic separation were water with 0.1% formic

acid (A) and acetonitrile with 0.1% formic acid (B). Samples were desalted using a reverse-phase SYMMETRY C18 trap column (100 Å, 5 µm, 180 µm × 20 mm, Waters Corporation) at a flow rate of 8 µL/min for 2 minutes. Peptides were separated by a linear gradient (0.3 µL/min, 35 °C; 97%-60% mobile phase A over 90 minutes) using an Acquity UPLC M-Class Reversed-Phase system (1.7 µm Spherical Hybrid, 76 µm × 250 mm, Waters Corporation).

Data were processed using MassLynx v4.1 and ProteinLynx Global Server 3.0.3 (both Waters Corporation) and searched using the human Uniprot database UP000005640 (version modified May 10, 2020). The database search was performed with the following parameters: mass tolerance was set to software automatic values; enzyme was specified as trypsin; up to 2 missed cleavages; cysteine carbamidomethylation was as a fixed modification plus several common variable modifications; 1% protein false discovery rate.

2.3 | Cleavage of β2GPI

Purified β2GPI was cleaved overnight using plasmin (Cambridge Biosciences) at a 1:1 ratio in cleavage buffer (100 mM Tris, 0.02 M NaCl, 0.3 mM CaCl₂, pH 7.5). Volumes were made up to 500 µL and left rotating overnight at 37 °C. Cleavage was confirmed through reduction studies. A total of 10 µL of reaction mix was incubated with 0.05 M Tris (2-carboxyethyl) phosphine hydrochloride or 0.1 M dithiothreitol for 15 minutes at 95 °C before being run on a 4% to 12% SDS-PAGE BOLT Gel (Invitrogen) for 32 minutes at 165 V. Samples that did not alter their migration under reduction were confirmed to be successfully cleaved. Note: batches of plasmin vary in activity; as such, each new batch was titrated using its stated activity rather than mg/mL; we identified that a 1:1 ratio generally overcame these variations, yielding plasmin-clipped β2GPI reliably.

2.4 | Dynamic light scattering

The hydrodynamic diameter of β2GPI at 0.1 mg/mL was measured using a Zetasizer Nano-ZS (Malvern Instruments). Samples were prepared by filtration (0.2 µm) and centrifugation (16 000 × g, 10 minutes) to reduce potential aggregate formation. Measurements were taken with a detector angle of 90° and a refractive index of 0.01. The pedestal height was allowed to float during measurements, ensuring a maximal signal. A total of 3 measurements per protein (6 runs with a duration of 10 seconds per measurement) were obtained, and data were averaged. Data were analyzed using Microsoft Excel, and statistical differences were derived using GraphPad Prism 7.0.

2.5 | SAXS

X-ray scattering data were obtained during a single beam session on Instrument B21 at the Diamond Light Source at the Harwell Science and Innovation Campus in Oxfordshire, operating with a ring energy of 3

GeV and a beamline operational energy of 12.4 keV [34]. A PILATUS 2M detector (Dectris) with a resolution of 1475 × 1679 pixels (pixel size of 172 × 172 µm) was used with a sample-to-detector distance of 4.01 m, giving a Q range from 0.04 to 4 nm⁻¹ (where $Q = 4\pi \sin \theta / \lambda$; 2θ = scattering angle; λ = wavelength). The β2GPI samples, at concentrations between 1.5 mg/mL and 0.1 mg/mL, in buffer were loaded onto a 96-well plate that was placed into an European Molecular Biology Laboratory Arinax sample holder [35,36]. This measurement condition showed the β2GPI molecule as a hydrated structure in a high positive solute-solvent contrast [17]. An automatic sampler injected 30 µL of sample from the well plate into a temperature-controlled quartz cell capillary with a diameter of 1.5 mm. Datasets of 30 frames with a frame exposure time of 1 second each were acquired in duplicate as a control of reproducibility. Checks during data acquisition confirmed the absence of radiation damage. Buffer subtraction was carried out automatically. Analysis of Guinier, P(r), and Kratky plots was carried out using ScatterIV (BIOISIS) and GraphPad Prism 7.0.

2.6 | Molecular dynamics

The crystal structure coordinates of β2GPI (PDB ID: 1c1z) were prepared for molecular dynamics (MD) using Glycan Reader and Modeler [37–40] at the CHARMM-GUI website (<http://www.charmm-gui.org/>). Protonable residues were edited on CHARMM-GUI. Modifications to take account of the plasmin clipping of β2GPI were carried out *in silico* through the deletion of amino acids 318–326 in PyMOL. Both plasmin-clipped and healthy control (HC; nonclipped) β2GPI had full glycan chains added in accordance with the 4 biantennary glycans detected by Kondo et al. [41], which were assembled and packed using CHARMM-GUI [39].

Full simulation methodology can be found in the [Supplementary Methods](#). In brief, simulations were carried out at 303.15 K for 100 nanoseconds using the CHARMM36 force field with NAMD. The convergence of the simulations for all systems was checked through the comparison of average root mean square deviation (RMSD) using visual molecular dynamics [42]. Each simulation was repeated 3 times, and the data were averaged for analysis. Simulations were run for >100 nanoseconds and yielded >3000 frames for analysis.

2.7 | Inhibition enzyme-linked immunosorbent assay

Inhibition enzyme-linked immunosorbent assays (ELISAs) were performed as previously described [26]. Briefly, serum samples with historical positivity for anti-β2GPI antibodies were tested in an anti-β2GPI ELISA. Maxisorp plates (Thermo Fisher Scientific) were coated with 2 µg/mL of β2GPI (Enzyme Research Laboratories) overnight at 4 °C before being blocked with 2% BSA/PBS (Sigma) for 1 hour at 37 °C (150 µL per well). Plates were washed with PBS Tween (0.1%) 3 times before application of serum at a dilution of 1:50 in 1% BSA in PBS for 1 hour at room temperature (50 µL per well). Plates were again

washed, and antihuman IgG conjugated to horse radish peroxidase (Sigma) was applied at a titration of 1:2000. The plate was again incubated at room temperature for 1 hour. Plates were washed, and 100 μ L of 3,3', 5,5'-tetramethylbenzidine (KPL) was added and incubated for 15 minutes at room temperature before being stopped with 100 μ L of stop solution (1 N, KPL). Plates were read by absorbance at 450 nm in a plate reader (Tecan Infinite PRO+, Tecan). Inhibition assays were performed identically with the exception of a 2-hour preincubation of serum samples with either HC (nonclipped) β 2GPI or plasmin-clipped β 2GPI at room temperature before application of the sample to the plate. Inhibition was calculated by comparing samples in the absence and the presence of inhibitors on a single plate.

2.8 | Native PAGE

Noncleaved protein was loaded at 0.6 μ g, 1.2 μ g, 2.4 μ g, and 5 μ g in a native loading buffer (Invitrogen). Plasmin-clipped β 2GPI was loaded at 5 μ g diluted in a native loading buffer (Invitrogen). Samples were loaded into a 10% Tris-Glycine Native PAGE Gel (Invitrogen) and run in Tris-Glycine Native Running Buffer (Thermo) at 150 V and variable milliamps for 5 hours at room temperature. Gels were transferred to PVDF membranes using the BioRad Turboblotter (7 minutes, 10 V mixed protocol) and blocked with 10% skimmed milk in phosphate buffered saline with Tween (PBST) (0.5%). The membrane was exposed to fluorescence (Thermo Fisher Scientific iBright) for Cy3 and Cy5. Membranes were then incubated with anti- β 2GPI antibody (PA-1-74015, Thermo Fisher Scientific) overnight. Membranes were washed with 10% milk in 0.5% PBST for 3 hours (3 \times 20 minutes) and then incubated for 1 hour, rolling at room temperature with anti-goat antibody conjugated to horse radish peroxidase (1:1000, DAKO). Finally, membranes were washed with PBST (0.5%) and exposed using Amersham Prime ECL (Amersham) on an Amersham ImageQuant 800 (Amersham, GE Healthcare).

2.9 | Fluorescent labeling and flow cytometry

Glycan labeling of β 2GPI was carried out using the N-Glycan Labelling Kit (BioTechne). Nonclipped β 2GPI was labeled using 1 μ L neuraminidase, 1 μ L StGal6, and 1 μ L of label per 5 μ g of protein and incubated at 37 $^{\circ}$ C for 1 hour. Clipped β 2GPI was labeled using 2 μ L neuraminidase, 2 μ L StGal6, and 5 μ L of label per 5 μ g of protein and incubated at 37 $^{\circ}$ C for 1 hour. Both labeled proteins were stored at 4 $^{\circ}$ C in the dark. Plasmin-clipped β 2GPI was labeled with Cy3, while nonclipped was labeled with Cy5. Labeled clipped and nonclipped β 2GPI were incubated with human umbilical vein endothelial cells (HUVECs) for 2 hours at 37 $^{\circ}$ C. Cells were plated at 500 000/well with 2 μ g of fluorescently labeled β 2GPI. Cells were incubated with Live/Dead Blue Viability Dye (Thermo Fisher Scientific) for 20 minutes in the dark at room temperature. Cells were then stained with CD105-BV421 (BioLegend, 43A3) for 30 minutes at 4 $^{\circ}$ C to allow identification of HUVECs and then incubated in fixation buffer

(Thermo Fisher Scientific) for 15 minutes at 4 $^{\circ}$ C in the dark. Percentages of cells positive for β 2GPI were then compared between plasmin-clipped β 2GPI and nonclipped β 2GPI. Samples were acquired on a Fortessa \times 20 flow cytometer (BD). Data were analyzed by FlowJo (v10).

2.10 | Ion mobility mass spectrometry

Ion mobility mass spectrometry (IMMS) was carried out in the Thalassinos Laboratory at University College London. Protein samples were buffer exchanged into 10 mM ammonium acetate using an Amicon (Merck) 30 kDa MWCO filter for analysis on a SELECT SERIES Cyclic IMS QToF (Waters Corporation) [43,44]. Samples were directly infused into the instrument at a concentration of 2.5 μ M using nano-electrospray capillaries prepared in-house using a Flaming-Brown (Sutter) P97 micropipette puller and gold-coated with a Quorum Q150RS (Quorum) sputter coater. Data were processed using UniDec and MassLynx v4.2.

3 | RESULTS

3.1 | Purity

Size exclusion chromatography of the final sample yielded a single peak; when analyzed by SDS-PAGE, it was the correct molecular weight for β 2GPI (Supplementary Figure S1A). Identification of β 2GPI was further confirmed using proteomics experiments, in which β 2GPI was identified with 76.8% sequence coverage despite being heavily glycosylated. Identity was further proved by solid phase assays (Supplementary Figure S1B-E) wherein the protein-bound APS patient antibodies were used in a specific manner. Proteomics analysis can also identify contaminant proteins to inform upon the purity of the protein preparation, identifying C8 proteins complement the C8 α and γ chains. The final purity calculated by densitometry (GelQuant) was 96% (lane 1, Figure 1A).

3.2 | Validation of cleavage of β 2GPI by plasmin

β 2GPI was cleaved successfully overnight (16 hours, 1:1 ratio), yielding approximately 50% cleaved protein. Confirmation of cleavage was achieved by SDS-PAGE (Figure 1A), and native PAGE/Western blot (Figure 1B) showed less shift for plasmin-clipped protein compared with nonclipped, mirroring findings by Matsuura et al. [17]. This effect may also be due to the modification of the terminal disulfide through cleavage, which has been shown previously to be preferentially reduced compared with the remaining 10 disulfides. In the native gel/Western blot, the plasmin-clipped protein forms a wider smear with higher mobility under native conditions, suggesting that it is more flexible and potentially more compact compared with the noncleaved linear structure. The affected sites from cleavage are

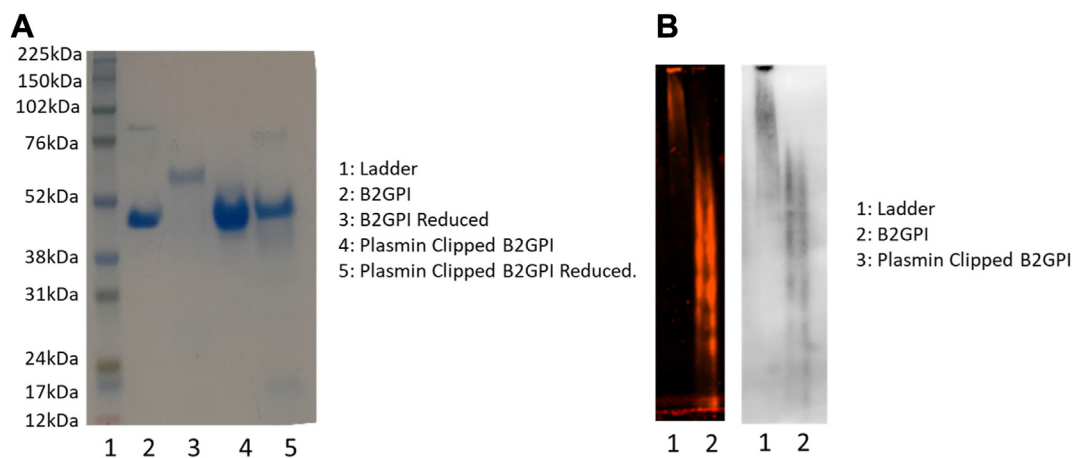


FIGURE 1 Production of plasmin-clipped β 2-glycoprotein I (β 2GPI). (A) Batches of protein were cleaved and confirmed for cleavage by reduction sodium dodecyl sulfate-polyacrylamide gel electrophoresis analysis. Whole β 2GPI, when reduced, has reduced mobility on a sodium dodecyl sulfate-polyacrylamide gel electrophoresis gel (lane 3); however, after cleavage, this reduced mobility is no longer seen (lane 5). (B) The fluorescently labeled β 2GPI and plasmin-clipped β 2GPI by native gel with the lower smear of structures representing the plasmin-clipped β 2GPI and the higher smear representing nonclipped β 2GPI. This was then probed with an anti- β 2GPI antibody, showing specificity on the right, highlighting a different structure in plasmin-clipped β 2GPI.

modeled in Figure 2. Masses were measured by mass spectrometry, with a smaller size seen in the plasmin clipped. Protein was purified from a plasmin mix using ion exchange chromatography, showing a shift in affinity under cation exchange conditions, eluting at a lower conductivity. This confirmed cleavage and enabled good separation of cleaved and noncleaved β 2GPI (not shown).

3.3 | Native IMMS data confirm the altered structure

Analysis of the nonclipped and clipped β 2GPI by means of native IMMS revealed differences between the 2 samples, both in the mass spectrometry and ion mobility dimensions. As shown in Figure 3A, multiple peaks can be seen for each charge state due to glycosylation,

demonstrating the considerable heterogeneity in both samples. While this is true for both samples, for the plasmin-clipped sample, there is a shift toward the lower charge states being more prominent, which is indicative of a more compact/folded conformation. This is shown further in the arrival time distributions (ATDs) obtained from the IM analysis. IM separates ions based on their interaction with a buffer gas as they travel through a mobility cell under the influence of a weak electric field. The time an ion takes to traverse the IM cell is related to its charge and rotationally averaged collision cross section (or Ω), the latter being a physical quantity related to the overall shape [45]. For ions of the same charge state, the more compact species will, therefore, have a faster ATD than an extended one. While the plasmin-clipped protein had 1 peak in the ATD, the nonclipped version had an additional, later-arriving peak, illustrating that the protein coexists in 2 broad conformers, a compact and an extended one.

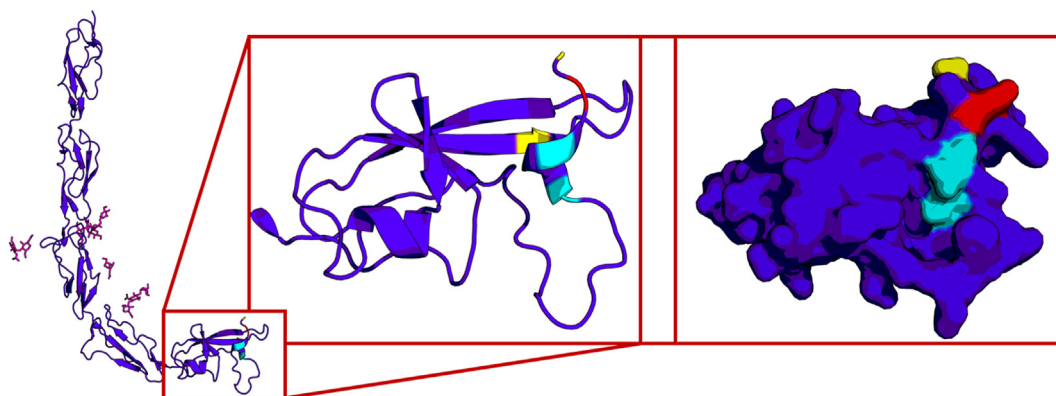


FIGURE 2 Altered charge and interactions. Plasmin cleavage removes the terminal 8 amino acids, leaving a truncated protein, the cleaved peptide being highlighted above in the Protein Data Bank model 1c1z. This peptide consists of 3 highly charged amino acids: 1 lysine (red) and 2 aspartic acids (cyan), while also containing a cysteine that forms part of an allosteric disulfide with the neighboring β -sheet (yellow). The partner cysteine is internal to the structure; as such, it has been highlighted in the ribbon model in yellow. Allosteric disulfides are associated with significant structural shifts; as such, the loss of the disulfide coupled with the alteration in local charge suggests it is likely that β 2-glycoprotein I undergoes a significant structural change postplasmin cleavage.

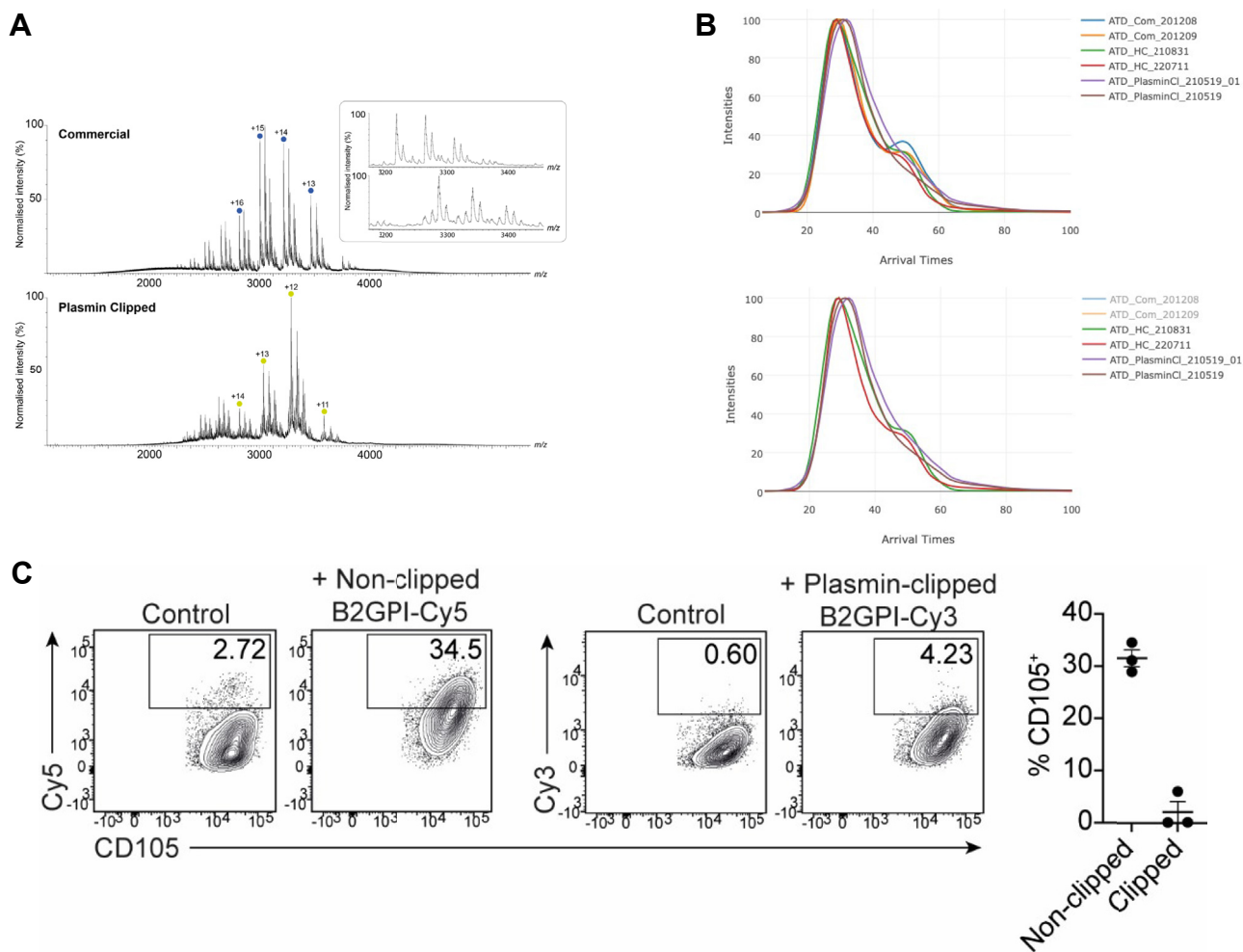


FIGURE 3 Ion mobility mass spectrometry and FACS analysis. (A) The spectra of both the nonclipped β 2-glycoprotein I (β 2GPI; top) and the plasmin-clipped β 2GPI (bottom), as can be seen, both retain a number of glycoisoforms; however, the Gaussian distribution of peaks is significantly different in the plasmin-clipped β 2GPI, suggesting a significant change. A significant shift in charge in the peaks is also seen, likely due to the removal of the terminal 8 amino acids containing significantly charged species (1 lysine and 2 aspartic acid residues). A zoom-in demonstrates the shift in species, again confirming that a modification has taken place. (B) Further to this, ion mobility data show that in nonclipped β 2GPI, there are 2 populations of structures, with the dominant structure being the earlier peak. In contrast, plasmin-clipped β 2GPI shows a single dominant structure, with the peak moving fractionally to the right, suggesting that cleavage not only removes 1 structure but may alter the remaining form. The top figure demonstrates commercial (Com) β 2GPI, healthy (HC) β 2GPI, and clipped β 2GPI, while the bottom selects just the HC and CI β 2GPI. The clipped β 2GPI is generated from this HC pool; as such, this comparison emphasizes the structural shift under cleavage conditions. Direct comparison of commercial and purified β 2GPI can be seen in [Supplementary Figure S3](#). (C) Plasmin-clipped β 2GPI is known to lose its ability to bind to cell surfaces; as such, we conducted FACS with fluorescently labeled β 2GPI (CI and nonclipped) on human umbilical vein endothelial cells. As can be seen, nonclipped β 2GPI (Cy5 labeled) bound to approximately 3% to 35% of cells (2 μ g β 2GPI, 500 000 cells) while plasmin-clipped β 2GPI bound between 0% and 4.5% of cells, which was significantly less. ATD, arrival time distribution; FACS, flow cytometry.

3.4 | Flow cytometry shows consistent activity

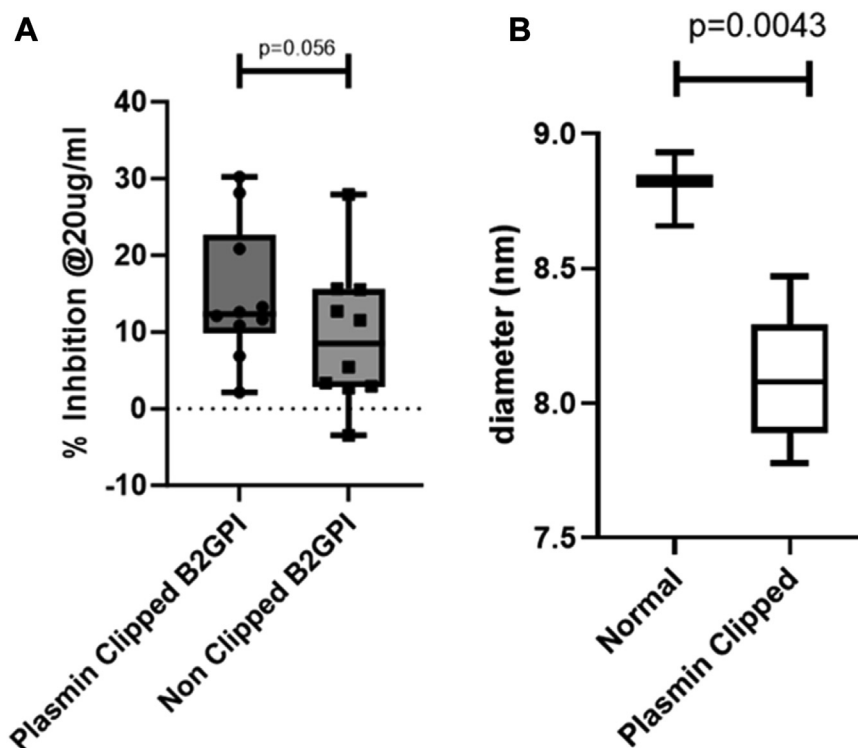
Noncleaved and plasmin-clipped β 2GPI were conjugated to Cy5 and Cy3, respectively, and incubated with HUVECs for 2 hours at 37 °C. HUVECs were stained with CD105-BV421 for identification by flow cytometry. Significantly higher frequencies of CD105⁺ HUVECs ($P < .05$) were positive for nonclipped β 2GPI (30%) compared with plasmin-clipped β 2GPI (<5%), consistent with findings from other studies [34–36]. The use of HUVECs in this experiment is based on previous research showing that the binding of β 2GPI to HUVECs utilizes the

same lysines as to negative surfaces; as such, this loss of binding confirms that cleavage has been successful and suggests that fluorophore labeling has not altered the physical function.

3.5 | ELISA assays

Activities of noncleaved and plasmin-clipped β 2GPI were measured using in-solution inhibition assays of patient serum. A total of 10 patients (8 female and 2 male) were used to test autoantibody binding to

FIGURE 4 Activity and structure. To test the activity of the plasmin-clipped β 2-glycoprotein I (β 2GPI) vs the nonclipped β 2GPI, we carried out competitive inhibitions using patient serum. Anti- β 2GPI positive serum was preincubated with 20 μ g/mL of either plasmin-clipped β 2GPI or nonclipped β 2GPI before exposure to a precoated β 2GPI enzyme-linked immunosorbent assay plate; a loss of binding to the plate was defined as an increase in inhibition by the in-solution inhibitors. (A) As can be seen, plasmin-clipped β 2GPI showed greater inhibition than nonclipped β 2GPI, suggesting a different structure with greater exposure to epitopes. (B) The dynamic light scattering profile of both the plasmin-clipped and nonclipped β 2GPI. As can be seen, the nonclipped β 2GPI has a higher dynamic radius, suggesting a larger defined structure, while the clipped β 2GPI shows a larger variation and a smaller size, suggesting the structure of plasmin-clipped β 2GPI is more flexible and smaller than nonclipped β 2GPI.



plasmin-clipped β 2GPI, and all 10 patients met the classification criteria [46] for APS. Patients were selected using a history of thrombosis and high anti- β 2GPI antibodies by clinical testing. While all patients had high α β 2GPI positivity, only 6 were triple positive (anti-cardiolipin, lupus anticoagulant, and α β 2GPI). In Figure 4A, the y-axis shows inhibition, defined as the percentage reduction in binding in the presence of an inhibitor (clipped or nonclipped β 2GPI) compared with the absence of an inhibitor. The mean inhibition was 14.9% (SD, 8.9%) for plasmin-clipped β 2GPI compared with 9.4% (SD, 9.1%) for non-clipped β 2GPI ($P = .056$). The high SD values are due to differences between patients in their overall α β 2GPI activity; however, as all samples were tested simultaneously with both inhibitors, the inhibition seen suggests an increase in binding in the plasmin-clipped form. This suggests that the structural alteration may influence the ability of β 2GPI to bind pathogenic antibodies in favor of the plasmin-clipped β 2GPI.

3.6 | Altered structural profiles after plasmin cleavage revealed by dynamic light scattering

Dynamic light scattering (DLS) measurements showed a significant difference ($P = .039$) in hydrodynamic radius between the plasmin-clipped β 2GPI ($n = 6$, 7.8 nm) and nonclipped β 2GPI ($n = 3$, 8.8 nm), Figure 4B. This difference of approximately 1 nm may be explained by a slightly different structural profile, with a smaller hydrodynamic radius accounting for a more compact form. This corresponds to the changes seen by native PAGE.

3.7 | SAXS comparison of plasmin-clipped and HC (nonclipped) β 2GPI

Plasmin-clipped and nonclipped β 2GPI were interrogated at the Diamond Light Source Facility in the Harwell Science campus (UK) for SAXS analysis. A range of concentrations from 1.5 mg/mL to 0.2 mg/mL were interrogated, with optimal comparative data being obtained for concentrations of 1 mg/mL. Buffer was subtracted automatically postnormalization, and no difference in intensity was seen between the 2 proteins (Figure 5A).

Guinier analysis was carried out on both HC and plasmin-clipped β 2GPI curves, identifying a single linear region (Figure 5B). The Q radius of gyration (R_G) limits were similar between both proteins, with the HC Q ranging from 0.446 \AA^{-2} to 1.287 \AA^{-2} while plasmin-clipped was 0.571 \AA^{-2} to 1.297 \AA^{-2} . These ranges were selected as they gave the most linear fit, and the inclusion of values up to a $Q R_G$ of 1.3 is in line to include globular, disk-, and rod-shaped objects. The R_G was calculated to have values of 40.9 \AA and 40.3 \AA for HC and plasmin-clipped β 2GPI, respectively.

Pair-distance distribution function analysis $P(r)$ was used to provide structural information in real space, where the largest Q value was limited to 0.13 nm^{-1} . D_{\max} was set to 118 nm for both proteins by trial and error, giving the smoothest descent to zero, and some slight aggregation was seen in the plasmin-clipped sample at very low Q values; however, this region was before the Q values used in the Guinier analysis. R_G values from the $P(r)$ analysis were smaller than for the Guinier analysis, with HC (nonclipped) calculated at 38.4 \AA while plasmin-clipped was calculated at 37.6 \AA . These values are within 10% of the Guinier analysis values and predict a smaller R_G for plasmin-

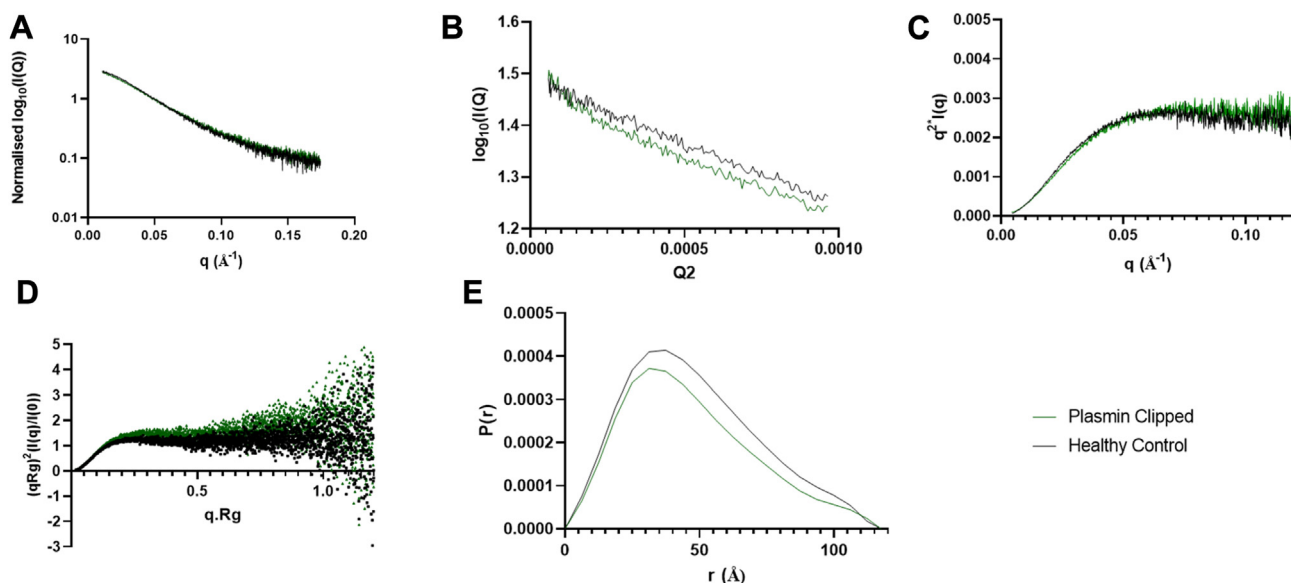


FIGURE 5 Small-angle X-ray scattering of plasmin clipped (green) and healthy control (nonclipped; black) purified β 2-glycoprotein I (β 2GPI). (A) the $\log I(Q)$ curve of both proteins; the peaks are at a similar point, suggesting they are both folded similarly; however, the green line maintaining a higher plateau may suggest increased flexibility in the plasmin-clipped β 2GPI. (B) A Guinier plot shows no significant difference between the proteins, while the (C) and (D) show Kratky plots (D being dimensionless) with the plasmin clipped showing a more defined peak and trending above the nonclipped, demonstrating increased flexibility (E) the $P(r)$ curve, with a characteristic high peak and extended tail in more rod-shaped structures, while the uneven shoulder shows the multidomain nature of the protein.

clipped β 2GPI, which is consistent with the DLS data. The peaks seen in the $P(r)$ analysis are formed by the most frequently occurring atomic distances within the structure; the dominant peak in both HC (nonclipped) and plasmin-clipped β 2GPI occurs between 30 and 40 Å, while the shape of the peak suggests a long rod shape. The maximum length of the protein (L) was calculated using the $P(r)$ function, identifying the shape as a long rod and solving the equation for L [47]:

$$L = R_G \sqrt{\frac{1}{12}}$$

This gave a length of 132.8 Å for HC β 2GPI and 130.2 Å for plasmin-clipped β 2GPI, again suggesting a smaller size for plasmin-clipped β 2GPI. Analysis of Kratky plots (Figure 5C) showed a more defined maximum for the plasmin-clipped protein (green) compared with HC (nonclipped) β 2GPI (black), while a dimensionless Kratky plot showed both proteins had a multidomain profile (Figure 5D). This suggested a less linear, although not a fully compact, globular protein form. This may also point to increased flexibility in the plasmin-clipped β 2GPI.

Further to this, the $P(r)$ function (Figure 5E) showed the characteristics of an elongated protein, with an initially well-defined peak before a tail around 75 Å. Although both samples showed this profile, a difference was seen in the height of the peaks, suggesting that although the 2 proteins were extended, they were nonidentical in structure. Fitting for multiple theoretical structures (circular and linear) at a number of concentrations did not yield curves similar to the experimental data (Supplementary Figure S4).

3.8 | MD

To generate potential model conformations that could explain the SAXS data, three 100 nanosecond repeats of MD simulations were run beginning from the linear crystal form (PDB:1C1Z). These simulations were then used as sources of β 2GPI structures to generate theoretical SAXS curves (>6000) to identify those conformers that fit best to the SAXS data [48,49]. SASSIE (CCP-SAS) was used to generate the theoretical curves from structures, which were then analyzed for best fit to experimental data using a chi-squared filter. The top 100 structures were identified and plotted in red in Figure 6A. All structures associated with HC (nonclipped) β 2GPI (bottom) had a smaller range of R_G than the plasmin-clipped β 2GPI (top). The top 100 structures, highlighted in red, were significantly different in their R_G values ($P = .0001$), with those for HC (nonclipped) ranging from 42.3 to 46.7 nm, while those for plasmin-clipped ranged from 38.9 to 43.6 nm. This reflects the smaller values for plasmin-clipped β 2GPI seen in the DLS data.

These top 100 hits were aligned and overlaid to evaluate whether there was a single consistent structure associated with either the HC (nonclipped) or plasmin-clipped β 2GPI. As can be seen in Figure 6, HC (nonclipped, blue) had a consistently extended J-shaped linear form of the structure, as has been observed previously by a number of methods, including crystal structures [6], atomic force microscopy [7], and SAXS [3]. By contrast, the plasmin-clipped β 2GPI (beige) consistently gave a novel S-shaped linear form of the structure, which was, therefore, more compact than the J-form. When overlaid with each

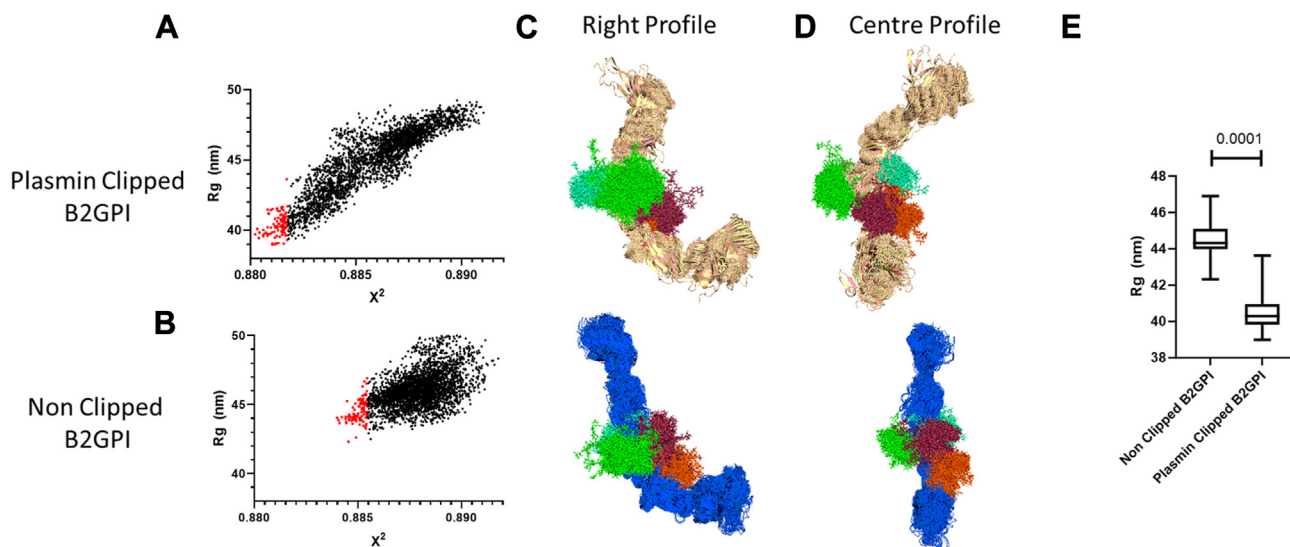


FIGURE 6 Analyzing the output from the small-angle X-ray scattering data using molecular dynamics with >3000 individual frames, we identified the top 100 fits for each structure from their respective simulation. (A and B) Plotting the radius of gyration (R_G) vs X^2 highlighted that the nonclipped β 2-glycoprotein I (β 2GPI) had structures with a higher R_G . (C and D) Further to this, visualizing the structures in PyMOL highlighted that the plasmin-clipped β 2GPI has a significantly different structure, with the first 2 domains (DI and DII) rotated. The green, red, orange and blue areas in the middle are the movements of the glycans (E) Plotting the best fitting 100 frames for both nonclipped and clipped β 2GPI showed a significantly higher R_G for nonclipped compared with plasmin-clipped β 2GPI, confirming what was seen by sodium dodecyl sulfate-polyacrylamide gel electrophoresis and ion mobility mass spectrometry.

other and aligned based on the third and fourth domains (DIII and DIV), there was a clear and significant divergence in the position of the first 2 domains (DI and DII; [Figure 6C, D](#)). The single best-fit models were then overlaid to show more clearly the difference ([Figure 6C, D](#)) between the 2 structures. The R_G was also significantly different, with smaller values seen in the plasmin-clipped β 2GPI, as shown in DLS, confirming that the SAXS and MD were consistent with other laboratory processes ([Figure 6E](#)).

Applying principal component (PC) analysis to the top 100 conformations of each of the HC (nonclipped) and plasmin-clipped β 2GPI showed a clear difference, with their structures clustering independently (hClust – hierarchical, complete linkage; [Figure 7C](#)). This was further demonstrated using aligned structures of best fit in [Figure 7A, B](#). All frames were trimmed to contain identical constructs that were aligned using all carbon atoms and PC analysis. Further to this, highlighting the DI epitope on a space model ([Figure 7D](#)) showed that the

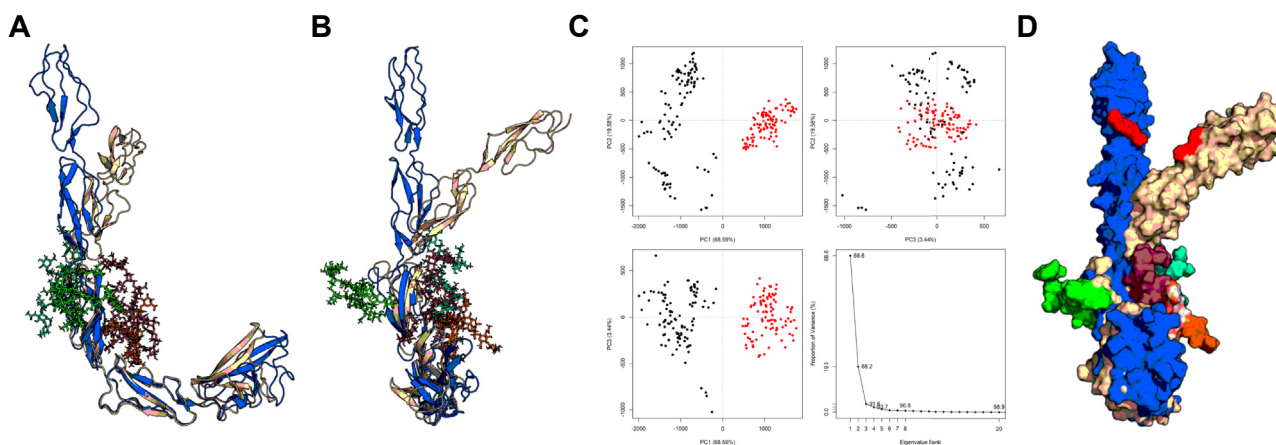


FIGURE 7 (A and B) Alignment of the best fitting structures from the molecular dynamics simulations by domain (D) IV (which shows the least difference) highlights the alterations in the orientation of DI and DII. (C) When combining the top 100 frames of each of the clipped and nonclipped β 2-glycoprotein I (β 2GPI) and conducting a principal component (PC) analysis, it shows that the 2 sets of structures are significantly different, with PC1 accounting for almost 70% of differences while PC2 accounts for another 19%, with the black dots being plasmin-clipped β 2GPI and the red dots nonclipped β 2GPI, also showcasing the high variability in structures in the plasmin-clipped β 2GPI compared with the nonclipped β 2GPI. (D) Finally, 2 space models of the best fits are overlaid with the R39-G43 epitope highlights. As can be seen, it is not simply a case of the protein bending, but in the plasmin-clipped β 2GPI, it also rotates, exposing the epitope differently, perhaps explaining the increased binding of antibodies in serum to the plasmin-clipped β 2GPI.

epitope has a potentially very different solvent exposure in the plasmin-clipped structure. Analysis of the entire simulations independently of the SAXS data showed a significantly increased RMSD for the plasmin-clipped β 2GPI over time. At the amino acid level, the regions of greatest movement, as measured by RMSD, were found in DI and DV (Figure 8A, B), as expected, with an open structure, with altered correlation between these amino acids. Measurement of interdomain regions highlighted significantly more movement in regions between domains III and DIV and DIV and DV (Figure 8C), suggesting the S shape may be due to alterations more proximal to the cleavage site. This also suggests that the switch to this novel S-shaped structure after cleavage by plasmin may be associated with an overall increase in flexibility within the protein as the terminal domains are both moving in opposition to one another. Furthermore, when clustering all conformations and not just the frames extracted from SAXS analysis and investigating the effect of each amino acid on the PCs, DV drives the separation in the first 5 PCs (Supplementary

Figure S1), suggesting this is driving the most significant structural change.

Plotting the other variables (RMSD/ R_G) for the top 100 fitted structures from the SAXS analysis identified structures with a high RMSD and a low R_G , suggesting they are flexible but compact, which links with the initial data from the DLS and native PAGE (Supplementary Figure S1C). Furthermore, these structures were found predominantly in the first cluster, which occurred early in the simulations, suggesting that they are quickly adopted and potentially, therefore, low energy.

4 | DISCUSSION

The role of plasmin-clipped β 2GPI is still a mystery in the context of APS, with little known about its structure and function. It has been shown that this β 2GPI cleavage can alter binding to negative surfaces

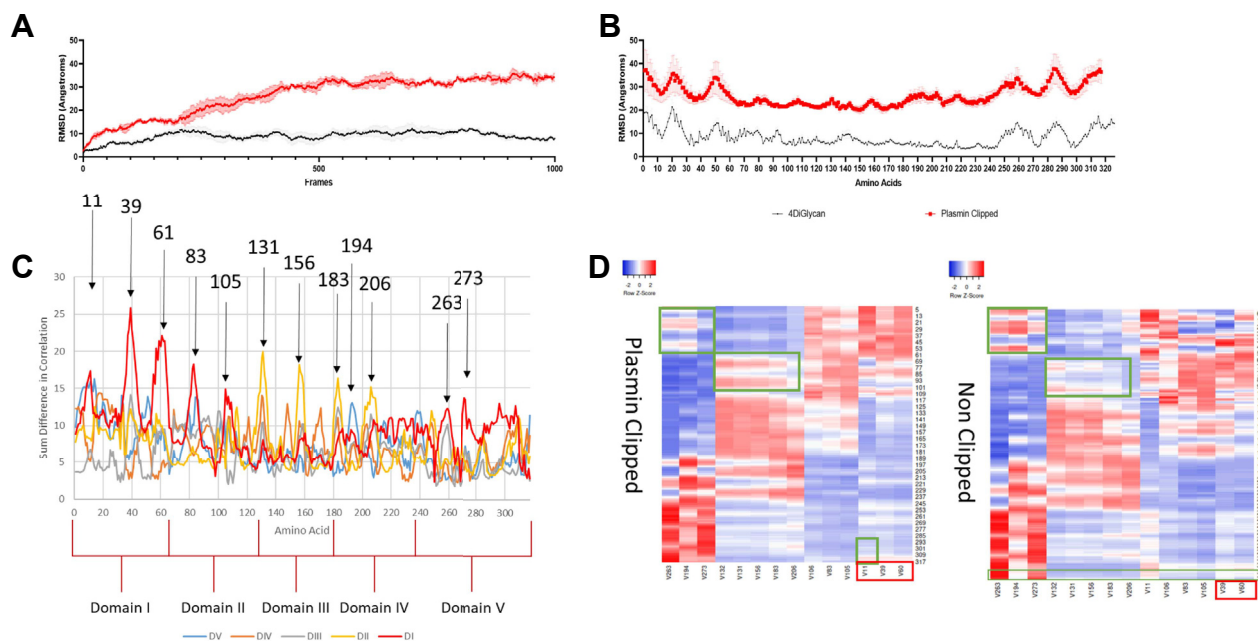


FIGURE 8 Further molecular dynamics analysis identified intraprotein networking that significantly differed across multiple domains (Ds) analyzed by DCCM matrixes. (A) This is demonstrated where sum differences in correlation per amino acid vs Ds are plotted. As can be seen, the red line (DI) shows the most significant changes in movement correlations with both itself and long-range to DV, similar to the yellow line (DII), which shows significant alterations in correlation with DIII and DIV. A number of amino acids are picked out as high points for variation, pointing to a pathway throughout the protein affected by the modification. (B) Plotting these variations on a heatmap of their correlation with other Ds and themselves reveals a backbone of amino acids that correlate with Ds throughout the protein. Interestingly, significant alterations are seen in how these amino acids signal together; the green boxes show areas where correlations are altered, with more correlations between V132 and V206 with DII in the plasmin-clipped model, whereas these are less strongly correlated in the nonclipped model. Similarly, DI correlates with V19, V273, and V194 strongly in the nonclipped model, but this is largely lost in the nonclipped model, suggesting this long-distance relationship is altered by clipping. The grouping of the amino acids themselves is changed, too, with V11 clustering more with DI in the plasmin-clipped model compared with the nonclipped model, which shows more correlation to later amino acids (V106-V206). (C) Further to this, we measured the root mean square deviation of the regions between each D. Decreased movement was seen between DI and DII, which correlates with what is seen in the small-angle X-ray scattering images, while increased movement is seen between DIII and DIV and DIV and DV. This corroborates what has been seen as increased flexibility in plasmin-clipped β 2-glycoprotein I and suggests that the increased binding of antibodies may be due to higher stability in the DI to DII regions. This lends credence to the idea that the cleavage of the terminal amino acids in plasmin clipped leads to an alteration in the movement of DI and DII relative to the rest of the protein, as seen in the previous experiments. Ns, not significant **** = $P < .01$, 4DiGlyc = nonclipped B2GPI; RMSD = root mean square deviation.

and alter the role β 2GPI plays in plasminogen generation [11,50]. However, its role in autoantibody binding is not fully understood [16].

The structure of β 2GPI is somewhat controversial. Agar et al. [1] proposed a linear (ie, J) and a circular (ie, O) form based on electron microscopy methods. More recently, other groups [4] have postulated that an S form exists, though it has not been proven. Most recently, the group of Pozzi interrogated β 2GPI using SAXS after molecular mutation to remove a disulfide bond in DV, showing a difference in structure [9]. Finally, Buchholz et al. [8] have shown structural change when lysines undergo posttranslational modification *in vitro*, resulting in an alteration of the linear-circular equilibrium. However, all of these modifications are *in vitro* and may not reflect exactly what occurs in patients. Plasmin cleavage has been confirmed to occur *in vivo* and is theorized to occur more frequently within APS patients. Given the role of clotting in disease progression and the role of β 2GPI in thrombosis and complement activation, which has been shown to be required for clotting in APS patients [2], it is fair to suggest plasmin-clipped β 2GPI does exist in APS patients *in vivo* and the lack of proof is a sign of the difficulties in assaying the molecule.

This study is the first to apply biophysical and computational methods to plasmin-clipped β 2GPI and has revealed a novel, potentially pathogenic structure of β 2GPI. It is difficult to directly corroborate a number of these methods; for example, the IMMS utilizes an approach capable of separating conformational families, while SAXS generates a structure based on an averaged ensemble approach; instead, these methods are best utilized together to define a broader underlying structural change. Traditional structural biology methods, such as DLS, suggested a compact variant of the linear structure of β 2GPI after plasmin cleavage. This was then corroborated by SAXS analysis, which highlighted structures with a smaller R_G and then revealed the S-shaped structure of plasmin-clipped β 2GPI by fitting the data to MD simulation structures. The simulation does, however, have the limitation of beginning from the linear form, thus biasing analysis to find noncircular forms. Similarly, although this manuscript shows the characteristic changes associated with plasmin cleavage, due to the change in charge, mass, and shape, we have been unable to confirm if the 8 amino acid peptide remains attached. Fitting for both the presence and absence of this did not significantly change the outcomes of the SAXS analysis. Similarly, although masses were derived for the major species of β 2GPI pre- and postcleavage, the masses were not perfectly aligned to the mass shift expected postcleavage; as such, further validation in other studies of these forms is required to understand potential other sites of cleavage. The structure identified in this study was associated with an increased ability to bind pathogenic autoantibodies from patients in serum as determined by ELISA, which has never been described previously for plasmin-clipped β 2GPI. Similarly, comparing different studies of β 2GPI is difficult as the preparation of β 2GPI and the method of measurement can lead to variation.

The identified novel conformation may also explain the unusual functions of plasmin-clipped β 2GPI (Supplementary Figure S2) as the different flexibility and surface exposures may alter affinity to binding partners. As discussed, plasmin-clipped β 2GPI can act as an inhibitor

of angiogenesis. However, this appears to be an enhancement of an inhibition activity already seen in the nonclipped β 2GPI. This enhancement may be due to the change in structural distribution between linear and circular β 2GPI caused by plasmin cleavage. It is also possible that due to the linked nature of thrombosis, fibrinolysis, and angiogenesis, this decreased angiogenic signal may be due to an alteration in one of the other pathways, for example, the loss of binding to plasminogen to convert to plasmin may alter the role plasmin plays in angiogenesis. Angiogenesis is not often explored in the setting of APS, as it is a coagulative disorder; however, APS antibodies have been shown to alter angiogenic processes in the endometrial space [51], and endothelial dysfunction is common in APS [52], which may, in turn, lead to angiogenic breakdown and potentially thrombus formation simultaneously.

Reed et al.'s [14] work on the potential for increased neonatal cardiac manifestations showed that β 2GPI was able to bind and sequester Ro60 when in its noncleaved form, mirroring the role of antiphospholipid antibodies in endothelial dysfunction [53]. However, the cleaved peptide generated in plasmin-clipped β 2GPI (consisting of 8 amino acids) may contain the sequence required for binding [14]. This directly points to conformational change altering the function of the protein. The effect of plasmin cleavage in cerebral infarct in APS patients is important as we have shown increased binding of pathogenic antibodies to plasmin-clipped β 2GPI. The mechanism behind this activity is incompletely understood with plasmin-clipped β 2GPI binding to Glu-plasminogen, whereas the nonclipped β 2GPI cannot. This leads to decreased fibrinolysis and, thus, increased clotting and is hypothesized to be through binding via the neutralized lysine cluster generated by a structural change first identified by Matsuura et al. [17]. This structural change in DV is confirmed in our work with the SAXS modeling, molecular simulation, and the lack of binding to cellular surfaces, implying a significant change in DV, including around the lysine-rich region. This also matches the work by Hoshino et al. [54], who identified similar changes using nuclear magnetic resonance. Interestingly, Hasdemir et al. [55] have recently completed an atomistic simulation of DV, highlighting the importance of these lysines within membrane binding, which corroborates the functions seen in our work.

To conclude, plasmin cleavage of β 2GPI resulted in a significant change in structure, yielding a novel S-shaped structure capable of increased antibody binding. This structure has increased flexibility and fits well with the literature showing an altered activity in plasmin-clipped β 2GPI compared with HC (nonclipped) β 2GPI. The demonstration of this new structure is an important step in understanding the functions of β 2GPI within the body.

ACKNOWLEDGMENTS

We thank Dr Felix Nagel for his insight in discussing the structure of β 2GPI during this project, and Dr Nathan Cowieson and Nikul Khunti for excellent user support on Beamline B21 at Diamond. We also thank Stephen McElvaney for his crucial role in logistical facilitation of this study. We also thank Dr Valentina Spiteri for her invaluable insight during drafting.

AUTHOR CONTRIBUTIONS

T.C.R.M. conceived and coordinated the study, carried out the experiments, and wrote the paper. H.F.B. recruited the patients, purified the cells and serum from them, and conducted flow cytometry experiments and analysis. C.J.L. helped perform the molecular dynamics simulations and small-angle X-ray scattering (SAXS) analyses. J.G. aided in the acquisition of data. X.G. assisted with the SAXS data collection. C.P. developed the original β 2-glycoprotein I inhibition assays and aided in their analysis. A.R. and I.G. provided the ethics permissions and patient samples. H.B. acquired ion mobility mass spectrometry data under the supervision of K.T. S.J.P. oversaw the SAXS analysis and helped write the manuscript. K.T., M.D., and P.A.D. helped with the study design, analytical development, and manuscript drafting.

DECLARATION OF COMPETING INTERESTS

T.C.R.M., C.P., I.G., and A.R. are inventors on a patent for the domain I of a β 2GPI-based therapeutic.

DATA AVAILABILITY

All data are contained within this manuscript and data are available on request.

ORCID

Hannah F. Bradford  <https://orcid.org/0000-0002-6827-3190>
 Christophe J. Lalaurie  <https://orcid.org/0000-0002-2085-6362>
 Xin Gao  <https://orcid.org/0000-0003-0877-0643>
 Charis Pericleous  <https://orcid.org/0000-0001-8804-0493>
 Stephen J. Perkins  <https://orcid.org/0000-0001-9218-9805>
 Konstantinos Thalassinos  <https://orcid.org/0000-0001-5072-8428>
 Ian Giles  <https://orcid.org/0000-0001-8913-3894>
 Anisur Rahman  <https://orcid.org/0000-0003-2346-4484>
 Mihaela Delcea  <https://orcid.org/0000-0002-0851-9072>
 Paul A. Dalby  <https://orcid.org/0000-0002-0980-8167>
 Thomas C.R. McDonnell  <https://orcid.org/0000-0002-1712-9957>

X

Thomas C.R. McDonnell  @McDonnellLab

REFERENCES

- Agar C, van Os GM, Mörgelin M, Sprenger RR, Marquart JA, Urbanus RT, Derksen RH, Meijers JC, de Groot PG. Beta2-glycoprotein I can exist in 2 conformations: implications for our understanding of the antiphospholipid syndrome. *Blood*. 2010;116:1336–43.
- McDonnell T, Wincup C, Buchholz I, Pericleous C, Giles I, Ripoll V, Cohen H, Delcea M, Rahman A. The role of beta-2-glycoprotein I in health and disease associating structure with function: more than just APS. *Blood Rev*. 2020;39:100610. <https://doi.org/10.1016/j.blre.2019.100610>
- Hammel M, Kriechbaum M, Gries A, Kostner GM, Laggner P, Prassl R. Solution structure of human and bovine β 2-glycoprotein I revealed by small-angle X-ray scattering. *J Mol Biol*. 2002;321:85–97.
- Pelkmans L, de Laat B. Antibodies against domain I of β 2-glycoprotein I: the one and only? *Lupus*. 2012;21:769–72.
- de Laat B, Derksen RH, van Lummel M, Pennings MT, de Groot PG. Pathogenic anti-beta2-glycoprotein I antibodies recognize domain I of beta2-glycoprotein I only after a conformational change. *Blood*. 2006;107:1916–24.
- Schwarzenbacher R, Zeth K, Diederichs K, Gries A, Kostner GM, Laggner P, Prassl R. Crystal structure of human beta2-glycoprotein I: implications for phospholipid binding and the antiphospholipid syndrome. *EMBO J*. 1999;18:6228–39.
- Buchholz I, McDonnell T, Nestler P, Tharad S, Kulke M, Radziszewska A, Ripoll VM, Schmidt F, Hammer E, Toca-Herrera JL, Rahman A, Delcea M. Specific domain V reduction of beta-2-glycoprotein I induces protein flexibility and alters pathogenic antibody binding. *Sci Rep*. 2021;11:4542. <https://doi.org/10.1038/s41598-021-84021-2>
- Buchholz I, Nestler P, Köppen S, Delcea M. Lysine residues control the conformational dynamics of beta 2-glycoprotein I. *Phys Chem Chem Phys*. 2018;20:26819–29.
- Kumar S, Chinnaraj M, Planer W, Zuo X, Macor P, Tedesco F, Pozzi N. An allosteric redox switch in domain V of β 2-glycoprotein I controls membrane binding and anti-domain I autoantibody recognition. *J Biol Chem*. 2021;297:100890. <https://doi.org/10.1016/j.jbc.2021.100890>
- Kumar S, Wulf J 2nd, Basore K, Pozzi N. Structural analyses of β 2-glycoprotein I: is there a circular conformation? *J Thromb Haemost*. 2023;21:3511–21.
- Bu C, Gao L, Xie W, Zhang J, He Y, Cai G, McCrae KR. Beta2-glycoprotein I is a cofactor for tissue plasminogen activator-mediated plasminogen activation. *Arthritis Rheum*. 2009;60:559–68.
- López-Lira F, Rosales-León L, Martínez VM, Ruiz Ordaz BH. The role of beta2-glycoprotein I (beta2GPI) in the activation of plasminogen. *Biochim Biophys Acta*. 2006;1764:815–23.
- Sakai T, Balasubramanian K, Maiti S, Halder JB, Schroit AJ. Plasmin-cleaved beta-2-glycoprotein 1 is an inhibitor of angiogenesis. *Am J Pathol*. 2007;171:1659–69.
- Reed JH, Clancy RM, Purcell AW, Kim MY, Gordon TP, Buyon JP. β 2-glycoprotein I and protection from anti-SSA/Ro60-associated cardiac manifestations of neonatal lupus. *J Immunol*. 2011;187:520–6.
- Yasuda S, Atsumi T, Ieko M, Matsuura E, Kobayashi K, Inagaki J, Kato H, Tanaka H, Yamakado M, Akino M, Saitou H, Amasaki Y, Jodo S, Amengual O, Koike T. Nicked β 2-glycoprotein I: a marker of cerebral infarct and a novel role in the negative feedback pathway of extrinsic fibrinolysis. *Blood*. 2004;103:3766–72.
- Hunt JE, Simpson RJ, Krilis SA. Identification of a region of beta 2-glycoprotein I critical for lipid binding and anti-cardiolipin antibody cofactor activity. *Proc Natl Acad Sci U S A*. 1993;90:2141, 15.
- Matsuura E, Inagaki J, Kasahara H, Yamamoto D, Atsumi T, Kobayashi K, Kaihara K, Zhao D, Ichikawa K, Tsutsumi A, Yasuda T, Triplett DA, Koike T. Proteolytic cleavage of beta(2)-glycoprotein I: reduction of antigenicity and the structural relationship. *Int Immunol*. 2000;12:1183–92.
- Smadja DM, Basire A, Amelot A, Conte A, Bièche I, Le Bonniec BF, Aiach M, Gaussem P. Thrombin bound to a fibrin clot confers angiogenic and haemostatic properties on endothelial progenitor cells. *J Cell Mol Med*. 2008;12:975–86.
- Alias S, Redwan B, Panzenboeck A, Winter MP, Schubert U, Voswinckel R, Frey MK, Jakowitsch J, Alimohammadi A, Hobohm L, Mangold A, Bergmeister H, Sibilia M, Wagner EF, Mayer E, Klepetko W, Hoelzenbein TJ, Preissner KT, Lang IM. Defective angiogenesis delays thrombus resolution: a potential pathogenetic mechanism underlying chronic thromboembolic pulmonary hypertension. *Arterioscler Thromb Vasc Biol*. 2014;34:810–9.
- Itoh Y, Inuzuka K, Kohno I, Wada H, Shiku H, Ohkura N, Kato H. Highly increased plasma concentrations of the nicked form of beta(2) glycoprotein I in patients with leukemia and with lupus

- anticoagulant: measurement with a monoclonal antibody specific for a nicked form of domain V. *J Biochem.* 2000;128:1017–24.
- [21] Kim SJ, Schneidman-Duhovny D, de Groot PG, Urbanus RT, Carter L, de Laat-Kremers R, Weiss TM, Chan MK, Sali A, Rand JH, de Laat B. Identification of thrombosis-related conformational binding epitopes on domain I of β 2-glycoprotein I. *Thromb Res.* 2024;237:145–7.
- [22] Brusca A. The significance of anti-beta-2-glycoprotein I antibodies in antiphospholipid syndrome. *Antibodies (Basel).* 2016;5:16. <https://doi.org/10.3390/antib5020016>
- [23] Pericleous C, Ruiz-Limón P, Romay-Penabad Z, Marín AC, Garza-García A, Murfitt L, Driscoll PC, Latchman DS, Isenberg DA, Giles I, Ioannou Y, Rahman A, Pierangeli SS. Proof-of-concept study demonstrating the pathogenicity of affinity-purified IgG antibodies directed to domain I of β 2-glycoprotein I in a mouse model of antiphospholipid antibody-induced thrombosis. *Rheumatology (Oxford).* 2015;54:722–7.
- [24] Pericleous C, Miles J, Esposito D, Garza-García A, Driscoll PC, Lambrianides A, Latchman D, Isenberg D, Rahman A, Ioannou Y, Giles I. Evaluating the conformation of recombinant domain I of β (2)-glycoprotein I and its interaction with human monoclonal antibodies. *Mol Immunol.* 2011;49:56–63.
- [25] McDonnell T, Pericleous C, Laurine E, Tommasi R, Garza-García A, Giles I, Ioannou Y, Rahman A. Development of a high yield expression and purification system for domain I of beta-2-glycoprotein I for the treatment of APS. *BMC Biotechnol.* 2015;15:104. <https://doi.org/10.1186/s12896-015-0222-0>
- [26] McDonnell TCR, Willis R, Pericleous C, Ripoll VM, Giles IP, Isenberg DA, Brasier AR, Gonzalez EB, Papalardo E, Romay-Penabad Z, Jamaluddin M, Ioannou Y, Rahman A. PEGylated domain I of beta-2-glycoprotein I inhibits the binding, coagulopathic, and thrombogenic properties of IgG from patients with the antiphospholipid syndrome. *Front Immunol.* 2018;9:2413. <https://doi.org/10.3389/fimmu.2018.02413>
- [27] Willis R, McDonnell TCR, Pericleous C, Gonzalez EB, Schleh A, Romay-Penabad Z, Giles IP, Rahman A. PEGylated domain I of beta-2-glycoprotein I inhibits thrombosis in a chronic mouse model of the antiphospholipid syndrome. *Front Immunol.* 2022;13:842923. <https://doi.org/10.3389/fimmu.2022.842923>
- [28] Albay A, Artim-Esen B, Pericleous C, Wincup C, Giles I, Rahman A, McDonnell T. Domain I of β 2GPI is capable of blocking serum IgA antiphospholipid antibodies binding in vitro: an effect enhanced by PEGylation. *Lupus.* 2019;28:893–7.
- [29] Salmon JE, Girardi G, Hokers VM. Complement activation as a mediator of antiphospholipid antibody induced pregnancy loss and thrombosis. *Ann Rheum Dis.* 2002;61(Supplement 2):ii46–50.
- [30] Serrano M, Martínez-Flores JA, Norman GL, Naranjo L, Morales JM, Serrano A. The IgA isotype of anti- β 2 glycoprotein I antibodies recognizes epitopes in domains 3, 4, and 5 that are located in a lateral zone of the molecule (L-shaped). *Front Immunol.* 2019;10:1031. <https://doi.org/10.3389/fimmu.2019.01031>
- [31] Pericleous C, Rahman A. Domain I: the hidden face of antiphospholipid syndrome. *Lupus.* 2014;23:1320–3.
- [32] Durigutto P, Grossi C, Borghi MO, Macor P, Pregnotato F, Raschi E, Myers MP, de Groot PG, Meroni PL, Tedesco F. New insight into antiphospholipid syndrome: antibodies to β 2glycoprotein I-domain 5 fail to induce thrombi in rats. *Haematologica.* 2019;104:819–26.
- [33] Cai G, Guo Y, Shi J. Purification of apolipoprotein H by polyethylene glycol precipitation. *Protein Expr Purif.* 1996;8:341–6.
- [34] Del Papa N, Sheng YH, Raschi E, Kandiah DA, Tincani A, Khamashta MA, Atsumi T, Hughes GR, Ichikawa K, Koike T, Balestrieri G, Krilis SA, Meroni PL. Human β 2-glycoprotein I binds to endothelial cells through a cluster of lysine residues that are critical for anionic phospholipid binding and offers epitopes for anti- β 2-glycoprotein I antibodies. *J Immunol.* 1998;160:5572–8.
- [35] Del Papa N, Guidali L, Spatola L, Bonara P, Borghi MO, Tincani A, Balestrieri G, Meroni PL. Relationship between anti-phospholipid and anti-endothelial cell antibodies III: beta 2 glycoprotein I mediates the antibody binding to endothelial membranes and induces the expression of adhesion molecules. *Clin Exp Rheumatol.* 1995;13:179–85.
- [36] Meroni PL, Del Papa N, Raschi E, Panzeri P, Borghi MO, Tincani A, Balestrieri G, Khamashta MA, Hughes GR, Koike T, Krilis SA. Beta2-glycoprotein I as a 'cofactor' for anti-phospholipid reactivity with endothelial cells. *Lupus.* 1998;7(Supplement 2):S44–7.
- [37] Jo S, Kim T, Iyer VG, Im W. CHARMM-GUI: a web-based graphical user interface for CHARMM. *J Comput Chem.* 2008;29:1859–65.
- [38] Jo S, Cheng X, Islam SM, Huang L, Rui H, Zhu A, Lee HS, Qi Y, Han W, Vanommeslaeghe K, MacKerell AD Jr, Roux B, Im W. CHARMM-GUI PDB manipulator for advanced modeling and simulations of proteins containing nonstandard residues. *Adv Protein Chem Struct Biol.* 2014;96:235–65.
- [39] Park SJ, Lee J, Qi Y, Kern NR, Lee HS, Jo S, Joung I, Joo K, Lee J, Im W. CHARMM-GUI glycan modeler for modeling and simulation of carbohydrates and glycoconjugates. *Glycobiology.* 2019;29:320–31.
- [40] Jo S, Cheng X, Lee J, Kim S, Park SJ, Patel DS, Beaven AH, Lee KI, Rui H, Park S, Lee HS, Roux B, MacKerell AD Jr, Klauda JB, Qi Y, Im W. CHARMM-GUI 10 years for biomolecular modeling and simulation. *J Comput Chem.* 2017;38:1114–24.
- [41] Kondo A, Miyamoto T, Yonekawa O, Giessing AM, Østerlund EC, Jensen ON. Glycopeptide profiling of beta-2-glycoprotein I by mass spectrometry reveals attenuated sialylation in patients with antiphospholipid syndrome. *J Proteomics.* 2009;73:123–33.
- [42] Humphrey W, Dalke A, Schulten K. VMD: visual molecular dynamics. *J Mol Graph.* 1996;14:33–8.
- [43] Eldrid C, Ben-Younis A, Ujma J, Britt H, Cragolini T, Kalfas S, Cooper-Shepherd D, Tomczyk N, Giles K, Morris M, Akter R, Raleigh D, Thalassinos K. Cyclic ion mobility-collision activation experiments elucidate protein behavior in the gas phase. *J Am Soc Mass Spectrom.* 2021;32:1545–52.
- [44] Eldrid C, Ujma J, Kalfas S, Tomczyk N, Giles K, Morris M, Thalassinos K. Gas phase stability of protein ions in a cyclic ion mobility spectrometry traveling wave device. *Anal Chem.* 2019;91:7554–61.
- [45] Gabelica V, Shvartsburg AA, Afonso C, Barran P, Benesch JLP, Bleiholder C, Bowers MT, Bilbao A, Bush MF, Campbell JL, Campuzano IDG, Causon T, Clowers BH, Creaser CS, De Pauw E, Far J, Fernandez-Lima F, Fjeldstedt JC, Giles K, Groessl M, et al. Recommendations for reporting ion mobility mass spectrometry measurements. *Mass Spectrom Rev.* 2019;38:291–320.
- [46] Miyakis S, Lockshin MD, Atsumi T, Branch DW, Brey RL, Cervera R, Derksen RHWM, de Groot PG, Koike T, Meroni PL, Reber G, Shoenfeld Y, Tincani A, Vlachoyiannopoulos PG. International consensus statement on an update of the classification criteria for definite antiphospholipid syndrome (APS). *J Thromb Haemost.* 2006;4:295–306.
- [47] Weiss TM. Introduction to small angle X-ray scattering; 2016. https://www.bing.com/search?q=Introduction+to+small+angle+X-ray+scattering&cvid=a99da8df56a3482998c006c00cc9c362&gs_lcrp=EgRIZGdIKyYIABBFdGkyBggAEEUYOTIGCAEQABhAMgYIAhAAGEAyBggDEAAyQDIGCAQQABhAMgYIBRAAGEAyBggGEAAyQDIGCAQQABhAMgYICBAAGEDSAQczODVqMGo5qAllsAIB&FORM=ANAB01&PC=DCTS. Accessed March 1, 2024. BioSAXS Workshop: online
- [48] Walker KT, Nan R, Wright DW, Gor J, Bishop AC, Makhatadze GI, Brodsky B, Perkins SJ. Non-linearity of the collagen triple helix in solution and implications for collagen function. *Biochem J.* 2017;474:2203–17.

- [49] Iqbal H, Fung KW, Gor J, Bishop AC, Makhatadze GI, Brodsky B, Perkins SJ. A solution structure analysis reveals a bent collagen triple helix in the complement activation recognition molecule mannan-binding lectin. *J Biol Chem.* 2023;299:102799. <https://doi.org/10.1016/j.jbc.2022.102799>
- [50] Ohkura N, Hagihara Y, Yoshimura T, Goto Y, Kato H. Plasmin can reduce the function of human beta2 glycoprotein I by cleaving domain V into a nicked form. *Blood.* 1998;91:4173–9.
- [51] Di Simone N, Di Nicuolo F, D'Ippolito S, Castellani R, Tersigni C, Caruso A, Meroni P, Marana R. Antiphospholipid antibodies affect human endometrial angiogenesis. *Biol Reprod.* 2010;83:212–9.
- [52] Velásquez M, Rojas M, Abrahams VM, Escudero C, Cadavid AP. Mechanisms of endothelial dysfunction in antiphospholipid syndrome: association with clinical manifestations. *Front Physiol.* 2018;9:1840. <https://doi.org/10.3389/fphys.2018.01840>
- [53] Andreoli L, Fredi M, Nalli C, Franceschini F, Meroni PL, Tincani A. Antiphospholipid antibodies mediate autoimmunity against dying cells. *Autoimmunity.* 2013;46:302–6.
- [54] Hoshino M, Hagihara Y, Nishii I, Yamazaki T, Kato H, Goto Y. Identification of the phospholipid-binding site of human beta(2)-glycoprotein I domain V by heteronuclear magnetic resonance. *J Mol Biol.* 2000;304:927–39.
- [55] Hasdemir HS, Pozzi N, Tajkhorshid E. Atomistic characterization of beta-2-glycoprotein I domain V interaction with anionic membranes. *bioRxiv.* 2024:585743. <https://doi.org/10.1101/2024.03.19.585743>, 2024.03.19.

SUPPLEMENTARY MATERIAL

The online version contains supplementary material available at <https://doi.org/10.1016/j.jtha.2025.02.015>